Effect of Shear Deformation on Convergability of Simple Contact Analysis with Large Displacement

***Z.M. Nizam[1], H. Obiya[2], K. Ijima[3], R. Tokubuchi[4], and K. Ishibashi[5]**

[1,4] School of Environmental Science and Engineering, Saga University, Japan.
[2,3,5] Department of Civil Engineering and Architecture, Saga University, Japan.
Saga University, Honjo 1, Saga City, Saga Prefecture, 840-8502, Japan.

*Corresponding author: mnizam@uthm.edu.my

Key Words: *Frictionless Contact Problem, Node-Element Contact, Critical Area, Shear Deformation, Tangent Stiffness Method, Pass-Through*

Abstract

A common problem encountered in the study of frictionless contact is the failure to obtain stable and accurate convergence result when the contact node is close to the element edge, which is referred as "critical area". In previous studies, we modified the element force equation to apply it to frictionless node-element contact problem using the Euler-Bernoulli beam theory (Tsutsui, Obiya and Ijima, 2009). A simple single-element consists two edges and a contact point was used to simulate contact phenomenon of a plane frame. The modification was proven to be effective by the convergability of the unbalanced force at the tip of element edge, which enabled the contact node to "pass-through", resulting in precise results. However, in another recent study, we discovered that, if the shear deformation based on Timoshenko beam theory is taken into consideration, a basic simply supported beam coordinate afforded a much simpler and more efficient technique for avoiding the divergence of the unbalanced force in the "critical area". Using our unique and robust Tangent Stiffness Method, the improved equation can be used to overcome any geometrically nonlinear analyses, including those involving extremely large displacements.

1 Introduction

The various methods and definitions that have been used to study contact problems in recent times have contributed numerous and interesting computation procedures. Previously studied contact phenomena involving large displacements analyses can be classified into four categories, namely contact between surfaces (Aliabadi and Martin, 2000; Rebel, Park and Felippa, 2002; Ayyad, Barboteu and Fernandez, 2009), contact between a node and a surface (Klarbing, 2002), contact between a node and an element (Chen, Nakamura, Mori and Hisada, 1998), and contact between elements (Konyukhov and Schweizrhof, 2010).

In this study, we developed a simple but effective method for studying the basic phenomenon of a node–element contact involving large displacements, and introduce a beam element comprising two edges and a contact point. We elaborate on the development of the method in Section 3. The idealization of the contact element produces a feasible contact phenomenon, which can be realistically computerized. This is illustrated by some numerical examples presented in this paper, in which accurate equilibrium of all nodes within the structure was achieved and the convergence of the unbalanced force was stable during each load increment.

To simulate extremely large deformation analyses, we used the tangent stiffness method (TSM), which produces very accurate and robust results for geometrically nonlinear analyses. Using this method, we formulated a simple but precise contact element without additional parameters or any complex derivation of the tangent geometrical stiffness and the element stiffness equation. Yet the method better satisfied the perfect equilibrium state than a common finite element method (FEM). The robustness is specifically shown in Section 4 as the numerical example 4.2 (Accuracy comparison of FEM to TSM), where a comparison of TSM to the study done by Konyukhov and Schweizrhof, 2010 using solid element by FEM. The study simulated the analysis of a large-deformation frictionless node–element contact of a cantilever beam, densely partitioned into 50 divisions. The comparison showed that the creation of such a large number of divisions is not necessary to obtain accurate results in TSM. Considering the discontinuity of the element boundary discussed by Chen and Nakamura (1998), an equilibrium state can hardly be achieved when the number of element increases. Conversely, TSM can be used to achieve stable convergence result without any concern with the density of mesh division.

In a node–element contact, it is difficult to achieve equilibrium when the contact node approaches the element edge owing to the nonconvergence of the unbalanced force. The sliding of the contact point toward element edges may reduce the l_i or l_j in Eqs. (5)-(8) to zero. This is due to a "division by zero" of the force equation matrices of the element given in Eq. (5), and it leads to the divergence of the unbalanced force. It should also be noted that the distance between the edges and the contact node are also the denominator of the matrices. To solve this problem, we used a shear deformation in Timoshenko beam as a countermeasure, including for slender beams. Furthermore, by introducing the shear deformation to the element force equation, the "critical area" where the unbalanced force hardly converges can be made significantly less than those of the Euler–Bernoulli beam, as shown in several examples.

We also studied the "pass-through" of a contact node using a simple algorithm for the inner and outer vector product, which produced stable convergence results, including at the tip of the element. In addition, the algorithm for the "pass-through" of the contact node to the next element was easier to implement and much more accurate at all the edges of the elements. In their work on frictionless node–element contact, Nizam, Obiya, and Burhaida (2008) proposed an algorithm that combines a contact element with the next noncontact element that the contact node is about to "pass-through". The equilibrium state was successfully achieved by this technique, although its reliability is low due to the change of mesh configuration, which affects the entire scheme. In another study (Tsutsui, Obiya and Ijima, 2009), an element force equation based on the cantilever beam coordinate was used to improve the "pass-through". The introduced equation enabled the convergence of the unbalanced force when the contact node was relatively close to the edge of the element—a configuration that had not been previously achieved. Furthermore, the findings of this study would facilitate further studies on node–element contact because its definitions and analytical results are precise, reliable, and very robust.

2 Tangent Stiffness Method

The TSM was solely idealized to overcome numerical cases exhibiting significant nonlinearity. The superiority of this method is that it converges the unbalanced force with high accuracy by defining element behavior using a simple form of the element

force equation. This theory requires the element edge forces to be treated separately and independently of each other. In addition, strict compatibility and an equilibrium equation are disseminated in the iteration configuration to converge the unbalanced force. This is equivalent to the Newton–Raphson method, which has an extremely high convergence performance.

2.1 General formulation

Here, an element has two edges and the force vector of both edges is assumed to be **S**. Considering a plane coordinate system, if the external force vector is denoted by **U**, and the equilibrium matrix by **J**, the equilibrium condition can be expressed by the following equation:

$$\mathbf{U} = \mathbf{JS} \tag{1}$$

By differentiating Eq. (1), the tangent stiffness equation can be expressed as

$$\delta\mathbf{U} = \mathbf{J}\delta\mathbf{S} + \delta\mathbf{J}\mathbf{S} = \left(\mathbf{K_O} + \mathbf{K_G}\right)\delta\mathbf{d} \tag{2}$$

Here, the differentiation of Eq. (1) simultaneously extracts $\delta\mathbf{S}$ and $\delta\mathbf{J}$, which enables the expression of a linear function of the displacement vector $\delta\mathbf{d}$ in the local coordinate system. Meanwhile, $\mathbf{K_O}$ represents the element stiffness matrix, which also simulates the element behavior corresponding to the element stiffness. $\mathbf{K_G}$ is the tangent geometrical stiffness.

Furthermore, a strict tangential stiffness equation can be obtained by a concise induction process without the use of a nonlinear stiffness equation. The induction process using a Lagrangian finite element is more complicated than the TSM.

3 Contact Problem

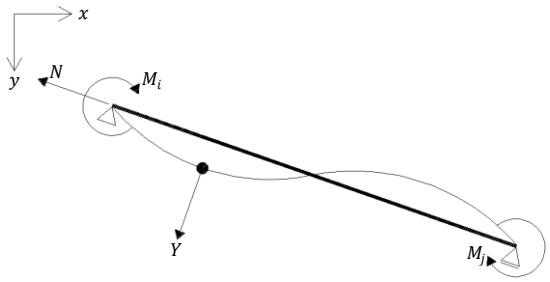

Figure 1: Element edge forces for contact element

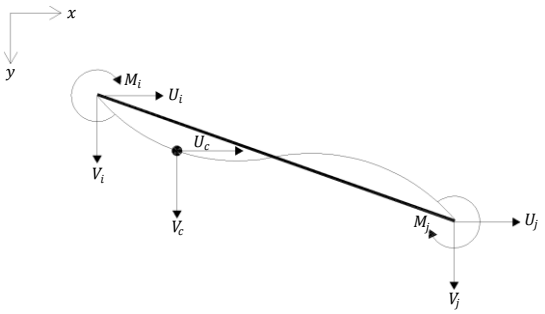

Figure 2: Nodal forces for contact element

A direct approach to frictionless contact between a node and an element using the Euler–Bernoulli and Timoshenko beams was developed and is presented in detail in this paper. A common equilibrium condition can be expressed for both theories as illustrated by means of a contact element in Figs. 1 and 2.

Fig. 1 shows the element edge forces for a single contact element, whereas Fig. 2 shows the nodal forces. The rotation of the contact node is neglected, which reduces the degree of freedom of the node to two. The vectors of the element edge force are independent of each other and are defined by the following equation:

$$\boldsymbol{S} = \begin{bmatrix} N & M_i & M_j & Y \end{bmatrix}^{\mathrm{T}} \tag{3}$$

Furthermore, the vector $\mathbf{U}$ can be expressed as follows:

$$\boldsymbol{U} = \begin{bmatrix} U_i & V_i & Z_i & U_j & V_j & Z_j & U_c & V_c \end{bmatrix}^{\mathrm{T}} \tag{4}$$

By differentiating Eqs. (3) and (4), the tangent geometrical stiffness can be obtained from the equilibrium between **S** and **U**.

3.1 Euler-Bernoulli beam theory using simply supported coordinate

Fig. 3 shows the equilibrium condition of an elastic and homogeneous simply supported beam under the action of the axial force $\boldsymbol{N}$, edge moments $\boldsymbol{M}_i$ and $\boldsymbol{M}_j$, and contact force $\boldsymbol{Y}_c$. Using the Euler–Bernoulli beam coordinate, it is assumed that the contact force $\boldsymbol{Y}_c$ is within the range of the beam, and that it produces the geometric and kinematic variables expressed in detail in the figure. This coordinate is a simple but accurate idealization of the frictionless node–element contact problem. The element force equations of this case are given as Eqs. (5) and (6).

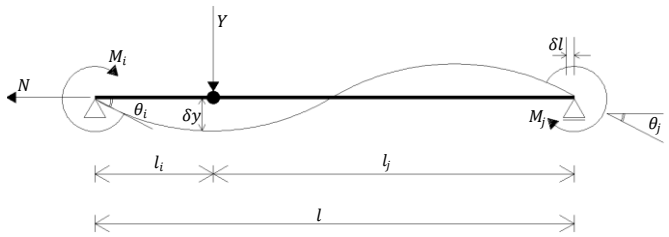

Figure 3: Contact problem in simply supported beam coordinate

$$\begin{bmatrix} N \\ M_i \\ M_j \\ Y_c \end{bmatrix} = \begin{bmatrix} \frac{EA}{l} & 0 & 0 & 0 \\ 0 & \frac{4l_{ic}+3l_{jc}}{l_{ic}}k_a & \frac{9l_0^{\,2}-l_{ic}^{\,2}l_{jc}^{\,2}}{l_{ic}^{\,2}l_{jc}^{\,2}}k_a & -\frac{3l_{jc}l_0^{\,2}}{l_{ic}^{\,2}l_{jc}^{\,2}}k_a \\ 0 & \frac{9l_0^{\,2}-l_{ic}^{\,2}l_{jc}^{\,2}}{l_{ic}^{\,2}l_{jc}^{\,2}}k_a & \frac{4l_{jc}+3l_{ic}}{l_{jc}}k_a & \frac{3l_{ic}l_0^{\,2}}{l_{ic}^{\,2}l_{jc}^{\,2}}k_a \\ 0 & -\frac{3l_{jc}l_0^{\,2}}{l_{ic}^{\,2}l_{jc}^{\,2}}k_a & \frac{3l_{ic}l_0^{\,2}}{l_{ic}^{\,2}l_{jc}^{\,2}}k_a & \frac{3l_0^{\,4}}{l_{ic}^{\,3}l_{jc}^{\,3}}k_a \end{bmatrix} \begin{bmatrix} \delta l \\ \theta_i \\ \theta_j \\ \delta y_c \end{bmatrix} \qquad k_a = \frac{EI}{l_0} \qquad (5), (6)$$

3.2 Euler-Bernoulli beam theory using cantilever coordinate

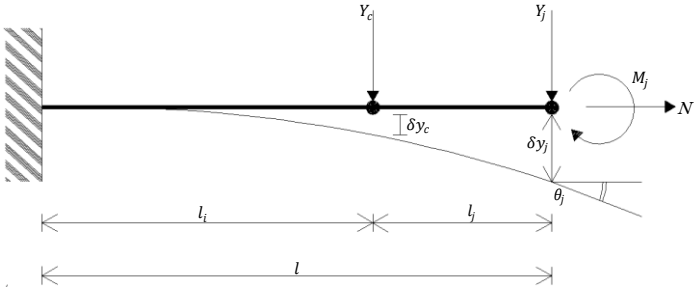

Figure 4: Contact problem in cantilever beam coordinate

$$\begin{bmatrix} N \\ Y_j \\ Y_c \\ M_j \end{bmatrix} = \begin{bmatrix} \frac{EA}{l} & 0 & 0 & 0 \\ 0 & l_i^{\,3}\left(l_i+4l_j\right)k_b & -ll_i^{\,2}\left(l_i+3l_j\right)k_b & -l_i^{\,3}l_j\left(l_i+2l_j\right)k_b \\ 0 & -ll_i^{\,2}\left(l_i+3l_j\right)k_b & l^4k_b & -ll_i^{\,2}l_jk_b \\ 0 & -l_i^{\,3}l_j\left(l_i+2l_j\right)k_b & -ll_i^{\,2}l_jk_b & \frac{l_i^{\,3}l_j^{\,2}\left(3l_i+4l_j\right)}{3}k_b \end{bmatrix} \begin{bmatrix} \delta l \\ \delta y_j \\ \delta y_c \\ \theta_j \end{bmatrix} \qquad k_b = \frac{3EI}{ll_i^{\,3}l_j^{\,3}} \qquad (7), (8)$$

The same Euler–Bernoulli beam is used in a cantilever coordinate system for a node–element contact. In this case, the existence of two concentrated forces; the contact force $\boldsymbol{Y}_c$ and the edge shear force act at the beam edge $\boldsymbol{Y}_j$, should be noted. In this coordinate, it is more likely to overcome the problem of "critical area" when the

distance between the contact node and the element edge is small, compared to the previous simply supported coordinate (Nizam, Obiya, and Burhaida (2008)). The element force equations (Eqs. (7) and (8)) can be easily used to execute a "pass-through" of the contact node to the next element. The equation for this coordinate system consists of the axial force $\boldsymbol{N}$, edge moment $\boldsymbol{M_j}$, contact force $\boldsymbol{Y_c}$, and the edge shear force $\boldsymbol{Y_j}$ which are independent to each other.

3.3 Timoshenko Beam Theory using simply supported coordinate

The fundamental assumption of the Euler–Bernoulli and the Timoshenko beam are the plane cross section remains plane. In Timoshenko beam, the cross section rotates due to the effect of shear deformation and no longer normal to the neutral axis. Furthermore, it is also assumed that the beam deformation is produced by two components, namely the bending and shear deformations (Fig. 5).

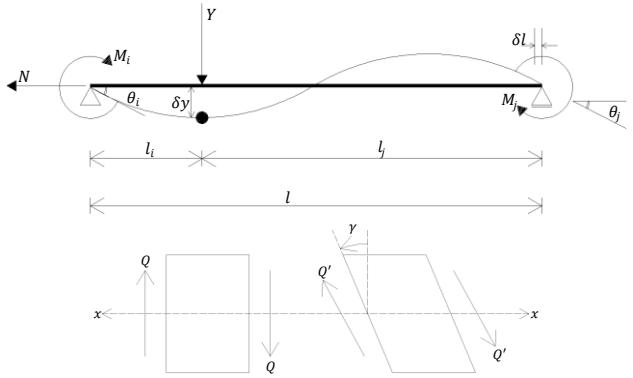

Figure 5: Effect of shear deformation in a beam

To simulate a contact phenomenon using the Timoshenko beam, a simply supported coordinate system can be used. The figure also reveals the existence of kinematic components, which were used in the previous Euler–Bernoulli beam (subsection 3.1).

$$\begin{bmatrix} N \\ M_i \\ M_j \\ Y_c \end{bmatrix} = \begin{bmatrix} \frac{EA}{l} & 0 & 0 & 0 \\ 0 & \left(4\Omega + 3l_{ic}{l_{jc}}^3 - 108\Psi^2\right)k_c & \left\{9\left({l_0}^2 - l_{jc}\Psi\right) - \Omega\right\}k_c & -3l_0\left(l_{jc}l_0 + 6\Psi\right)k_c \\ 0 & \left\{9\left({l_0}^2 - l_{jc}\Psi\right) - \Omega\right\}k_c & \left(4\Omega + 3{l_{ic}}^3 l_{jc} - 108\Psi^2\right)k_c & 3l_0\left(l_{ic}l_0 + 6\Psi\right)k_c \\ 0 & -3l_0\left(l_{jc}l_0 + 6\Psi\right)k_c & 3l_0\left(l_{ic}l_0 + 6\Psi\right)k_c & \frac{3l_0\left({l_0}^3 + 12l_0\Psi\right)}{l_{ic}l_{jc}}k_c \end{bmatrix} \begin{bmatrix} \delta l \\ \theta_i \\ \theta_j \\ \delta y_c \end{bmatrix} \quad (9)$$

$$k_c = \frac{EI}{l_0\Omega}, \qquad \Psi = \frac{EI}{GA_e}, \qquad \Omega = \left(l_{ic}l_{jc}\right)^2 + 3\Psi\left({l_0}^2 + l_{ic}l_{jc}\right) + 36\Psi^2 \qquad (10), (11), (12)$$

In this subsection, the element force equation of node-element contact for the Timoshenko beam is expressed as Eqs. (9)-(12). These equations are developed to overcome the "division by zero" discussed in section 1, to encounter the problem when the contact node approaches element edge into the "critical area" and leads to the divergence of unbalanced force. Furthermore, owing to the reduction of "critical area" enhanced by these equations, "pass-through" could be executed smoothly for the contact node to shift to the next noncontact element with stable convergence result. The effectiveness of these equations are demonstrated in details in each numerical examples in the following section.

4 Numerical Examples

4.1 Frictionless contact analysis of a cantilever beam

The main objective of this analysis is to investigate the range of the "critical area", by comparing the application of the Timoshenko beam in the element force equation (see Eqs. (9)–(12)) to the previous equations developed by Tsutsui, Obiya, and Ijima (2009). As shown in Fig. 5, the distances between the contact point and the two edges are l_i and l_j, respectively. In this case, if $l_i \rightarrow 0$ or $l_j \rightarrow 0$ in Eqs. (5) and (7), the matrices become singular. Therefore, if l_i or l_j is close to zero, the unbalanced force would hardly converge. This implies that there is a particular space close to the element edge in which the approach of the contact node is prohibited from achieving convergence result. We refer to this space as the "critical area".

As shown in Fig. 6, a cantilever beam configuration is used in this analysis, and the beam consists of 18 elements and 19 nodes. A compulsory displacement in the lateral upward direction is applied to the control node, which is independent and unconnected to any element in the primary position. The material parameters are $E = 2.1 \times 10^{11}$ [N/m^2], $A = 0.005$ [m^2], $I = 0.001$ [m^4], $G = 7.5 \times 10^{10}$ [N/m^2], and $\upsilon = 0.4$.

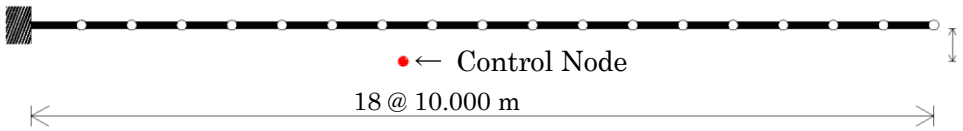

Figure 6: Cantilever beam model

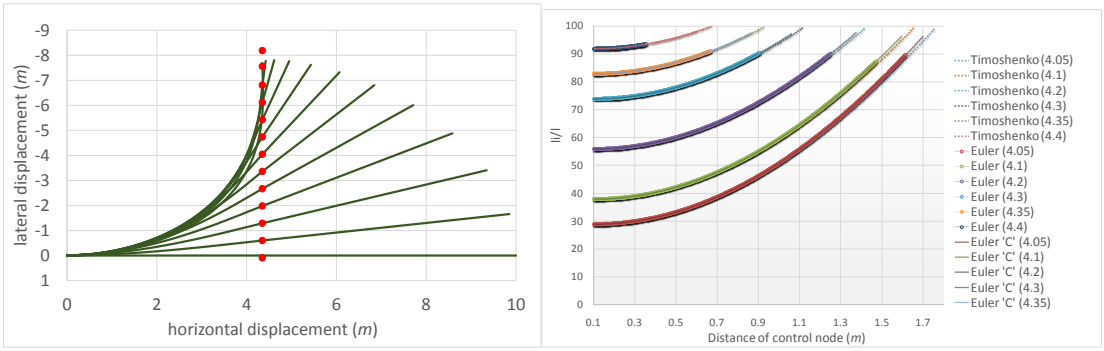

(a) **(b)**

Figure 7: (a) Beam deformation, (b) Comparison of "critical area" by three different element force equations

Fig. 7(a) shows the beam deformation due to the displacement of the control node, whereas Fig. 7(b) shows the relationship between the ratio l_i/l of a contact element and the displacement of the control node after contact. In this analysis, the control node was set at six primary positions, namely 4.05, 4.1, 4.2, 4.3, 4.35, and 4.4 m in the horizontal direction. The results of the analysis showed that the "critical area" of the Euler–Bernoulli beam in the simply supported coordinate system of Nizam, Obiya, and Burhaida (2008) ranged between 7.749% and 12.952%, whereas that of the cantilever coordinate system of Tsutsui, Obiya, and Ijima (2009) ranged between 2.164% and 3.865%. An idealization of the cantilever coordinate system by comparison of the two results can be used to reduce the range of the "critical area". However, using the Timoshenko beam, the "critical area" can be significantly reduced from 0.067% to 0.501%. The reduction of the "critical area" makes it easier

for the contact node to smoothly "pass-through" the element edge to the next element, producing a strict equilibrium solution.

4.2 Accuracy comparison of FEM to TSM

In this analysis, we compare the FEM of Konyukhov and Schweizrhof (2010) with the TSM for contact simulation. A cantilever beam with solid elements and 50 divisions was used for the FEM study, whereas simple linear elements are used for our TSM study. To demonstrate the accuracy of TSM, 10, 20, and 50 divisions of the beam are used in this study. The control node is displaced in the upper left direction by the vector [1, 0.6366], and the material parameters are $E = 2.1 \times 10^4$ [N/m^2], $b \times h = 0.02 \times 0.02$ [m], $L = 1.00$ [m], $G = 7.5 \times 10^{10}$ [N/m^2], and $\upsilon = 0.3$.

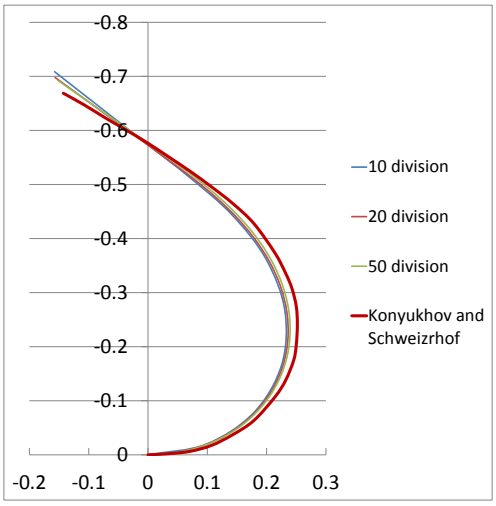

Figure 8: Beam deformation

Fig. 8 shows the beam deformation for both methods. The figure reveals that the beam deformations for TSM and FEM are not significantly different. The TSM solution for the larger 10 and 20 divisions is similar to that of FEM using densely partitioned solid elements. Furthermore, a simple definition of the contact element is sufficient to simulate the TSM contact analysis, while also avoiding the complex settings of the nonlinearity between the strain and the displacement.

4.3 Contact of double beams

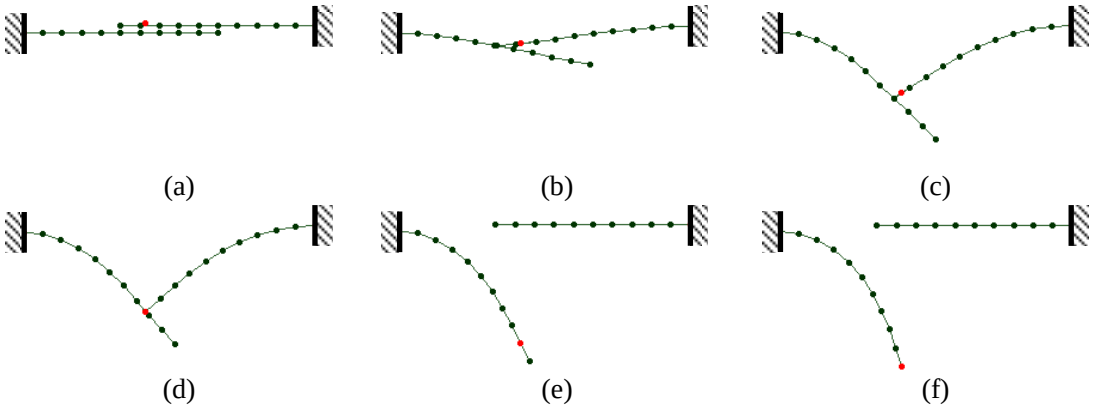

Figure 9(a)-(f): Control node displacement quantity and beams deformation

Two independent cantilever beams are used in this analysis, and the control node is displaced laterally and downward until it exceeds those of the two beams. The objective of this analysis is to perform multiple contacts using the Timoshenko beam, taking into consideration the "critical area", the "pass-through" phenomenon, and the deformation behavior of both structures. Both beams have 10 equal divisions, and the material parameters in this case are $E = 2.0 \times 10^7$ [N/m^2], $A = 3.0 \times 10^{-4}$ [m^2], $I = 2.2 \times 10^{-8}$ [m^4], $G = 7.142 \times 10^6$ [N/m^2], and $\upsilon = 0.4$.

Contact is about to occur when the displacement of the control node is at stage (a). At stage (b), multiple contacts initially occur between the control node and an element of the upper beam, and between the tip of the upper beam and an element of the lower

beam. The control node is displaced until stage (d), at which time the control node is about to shift from the upper beam and make contact with an element of the lower beam. The analysis is continued until the control node displacement is at stage (f), when the node is about to exceed the lower beam. By applying the Timoshenko beam, the significant reduction of the "critical area" discussed in Subsection 4.1 enables the contact nodes to smoothly and simultaneously "pass-through" every element edge.

5 Conclusion

The application of proposed contact element enables feasible node-element contact with large displacement. Based on the findings of this study, we make the following conclusions:

1) The convergence of the solution observed in the numerical analyses shows the effectiveness of the idealization of applying shear deformation of Timoshenko beam. Smooth "pass-through" solves the problem associated with discontinuous element boundaries. In addition, the reduction of "critical area" at every element edges to 0.067% facilitated the converged solutions.
2) The proposed contact element shows a very high performance with the usage of less element division and adequate if compared to the application of solid element. Furthermore, this is a significant merit in order to reduce the cost of calculation thus, it is practical to be deal with.
3) Regarding to the decrement of the range of "critical area", the provided numerical example 4.3 shows multiple contact phenomena could be executed at the same time. All of the contact nodes were able to "pass-through" smoothly without any divergence of the unbalanced force.

References:

Aliabadi, M. H.; Martin, D. (2000): Boundary element hyper-singular formulation for elastoplastic contact problems. *International Journal for Numerical Methods in Engineering*, vol. 48, pp. 995–1014.

Rebel, G.; Park, K. C.; Felippa, C. A. (2002): A contact formulation based on localized Lagrange multipliers: formulation and application to two-dimensional problems. *International Journal for Numerical Methods in Engineering*, vol. 54, pp. 263–297.

Ayyad, Y.; Barboteu, M.; Fernandez, J. R. (2009): A frictionless viscoelastodynamic contact problem with energy consistent properties: Numerical analysis and computational aspects. *Computer Methods in Applied Mechanics and Engineering*, vol. 198, pp. 669–679.

Klarbring, A. (2002): Stability and Critical Points in Large Displacement Frictionless Contact Problems. *J.A.C. Martins and M. Raous (Eds.) Friction and Instabilities*, Springer 2002, no. 457, pp. 39–64.

Chen, X.; Nakamura, K.; Mori, M.; Hisada, T. (1998): Finite Element Analysis for Large Deformation Frictional Contact Problems with Finite Sliding. *The Japan Society of Mechanical Engineers*, vol. 64, pp. 50–57.

Z. M. Nizam; H. Obiya; B. Burhaida. (2008): A study on non-friction contact problem with large deformational analyses. *Malaysian Technical Universities Conference on Engineering and Technology*.

T. Tsutsui; H. Obiya; K. Ijima. (2009): An algorithm for contact problem with large deformation of plane frame structures. *Advances in Computational Engineering & Sciences*.

Konyukhov, A.; Schweizerhof, K. (2010): Geometrically exact covariant approach for contact between curves. *Computer Methods in Applied Mechanics and ENgineering*, vol. 199, pp. 2510–2531.

Alexander, T., Marco, S., Marco, G., (2007): *Refinement of Timoshenko Beam Theory for Composite and Sandwich Beam using Zigzag Kinematics*. National Aeronatics and Space Administration (NASA).